

# Beam-Steered Optical Wireless Communication based on Piezoelectric Actuators and Micro-Lenses

Eduardo Muller<sup>(1)</sup>, Yuchen Song<sup>(1)</sup>, Ton Koonen<sup>(1)</sup>, Eduward Tangdiongga<sup>(1)</sup>

(1) Electro-Optical Communication Systems, Electrical Engineering, Eindhoven University of Technology, 5612 AP, Eindhoven, The Netherlands, [e.muller@tue.nl](mailto:e.muller@tue.nl)

## Abstract.

We demonstrate fast beam-steering in an OWC system by moving the optical source in the focal plane of a micro-lens using a pair of piezoelectric actuators. We achieved angles of 28° in the horizontal and 13° in the vertical axis, with 1.25 Gbps transmission rate. ©2023 The Author(s).

## Introduction

Data consumption is growing rapidly, leading to overloads on wireless network infrastructures. The limited number of legally defined frequencies, combined with overcrowding due to the internet-of-things (IoT) [1], exacerbates the problem of congestion experienced by users. To address this problem, we propose to use optical wireless communication (OWC) technology, which can off-load traffic from RF frequencies [2]. OWC has numerous advantages over traditional radio-wireless communication [3], including huge bandwidths, low latency, high privacy and security, and almost no interference from neighboring wireless networks.

In the development of an indoor network, we propose a transmitter that can track and connect to multiple mobile users. To achieve the optimum data throughput, it is necessary for an optical antenna to deliver maximum optical power to each receiver. However, due to eye safety concerns [4], the beam power must not exceed the safety threshold. As a result, the optical beams should be shaped such that only users asking for communication are served by these narrow optical beams. Hence, no optical power is wasted and a maximum quality of service can be delivered to wireless users while respecting eye safety [5].

The exact location of users must be known by the OWC system so that the optical beams can individually be directed to users in order to ensure proper alignment with the user's receiving aperture. Fig. 1 illustrates an indoor OWC use case [6] addressed in this work. The fiber-to-the-room (FTTR) technology connects a residential gateway (RG) to various users via the ceiling installed pencil radiating antennas (PRAs), see Fig. 1a. We used the wavelength domain to transport data to/from the RG.

In a PRA, a beam steerer is required to direct the optical beam to a desired angle where users are located. There are already several steering concepts that have been realized in laboratory setups and demonstrators.

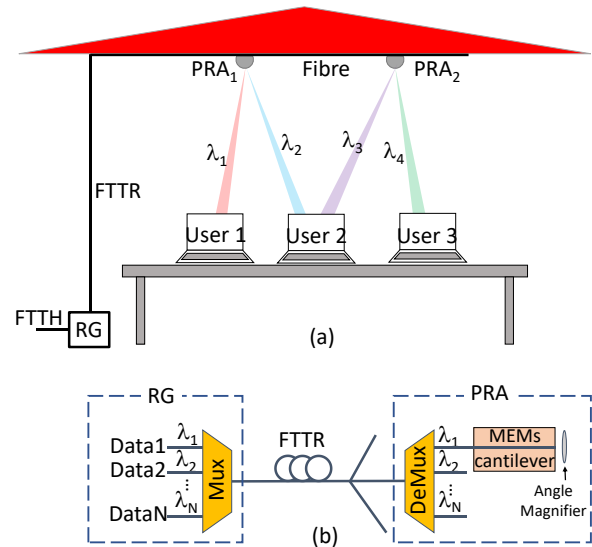


**Fig. 1:** Indoor optical wireless serving different users. (a) concept of fiber-to-the-room with last meters using narrow optical beams. (b) Link topology from RG to the ceiling PRA that employs MEMS cantilever with piezo actuators to steer the beams.

Among them are polarization gratings [5], arrayed waveguide grating routers [6], micro-electromechanical systems (MEMs) [7], metasurfaces [8], optical phased arrays [9], and spatial light modulators [10]. All these solutions can steer the optical beams with varying key performance aspects and one of them is power efficiency. This power efficiency is largely related to the optical losses.

Our concept uses MEMs cantilevers which are activated by piezoelectric actuators [7], which do not affect the optical signal properties because only the fiber tip is moved. The movement is magnified by micro-lenses [11], which can increase the steering angle considerably in order to cover a sufficiently large wireless area. Additionally, these compact actuators can be arranged in an array to accommodate multiple users simultaneously.

## Experiments

Fig. 2(a, b) shows respectively the schematic diagram of the experimental setup and the layout

of the realized 2D MEMs cantilever including the control pads for vertical and horizontal actuation.

An Anritsu pulse pattern generator (MP1701A) creates the pseudo-random binary sequence (PRBS-9) to drive directly a laser which is centered at  $\lambda=1561$  nm, emitting 5.6 dBm optical power, amplified to 13dBm by an Amonics optical fiber amplifier (EDFA). An external clock is used, with the pulse created by a Rohde & Schwarz Signal Generator (SME 02) defining the bitrate of the system.

The intensity-modulated light is coupled into the MEMs cantilever module where the fiber optical source is fixed (see Fig. 2b). The MEMs cantilever is driven by x- and y-actuators to a desired direction or transmission angle. At the output before free-space transmission over 40 cm, a micro-lens is located to increase the scan angle of the cantilever. The scan angle is measured on an infrared sensitive screen relative to the center of the optical beam.

In addition to scan range measurement, we performed bit-error rate measurements to evaluate the optical link quality performance for different scan angles. Therefore, we replaced the screen with a wide field of view (FoV) OWC receiver. It should be noted here that since the light after the cantilever and lens is largely collimated, the free space link length can reach much higher values than reported in this work. Moreover, since we are interested to know the beam performance when steering the beam to several angles relative to the normal angle, we employed a narrow bandwidth (around 750 MHz) but wide FoV ( $20^\circ$  full angle) OWC receiver [2] and measured the difference in the receiver sensitivity.

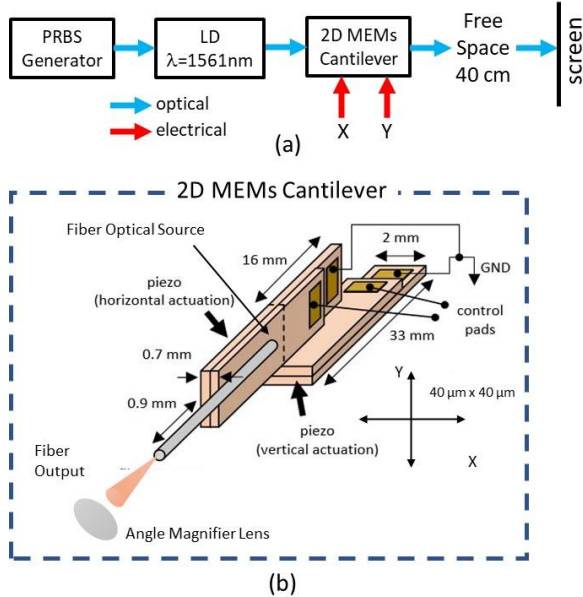


**Fig. 2:** (a) Experimental setup to test the beam steerer and (b) 2D MEMs cantilever with piezoelectric actuators. For BER evaluation, the screen is replaced by an OWC receiver followed by a BER tester.

The output fiber connected to the laser is then moved by a pair of commercial bimorph piezoelectric actuators [7], which are controlled by a pair of variable power supplies ranging from 0 to +25V. The voltage was limited at 20V for the horizontal movement and 24V for the vertical, to keep the beam inside the FoV ( $28^\circ$  horizontally and  $23^\circ$  vertically) of the measuring equipment. The single-mode fiber is terminated with a lens of 7.5  $\mu$ m diameter, which when used in conjunction with the micro-lenses, it produces a better collimated beam, with a beam divergence of  $4.4^\circ$ .

The actuators and fiber were mounted on a ThorLabs 3-axis MicroBlock (MBT616D/M), which can perform a precise adjustment of the actuators (1- $\mu$ m resolution) and fiber in relation to the lenses. Then the lenses were placed in a 6-axis optics mount (K6XS) at the crystal holder (K6A1/M). After the system is aligned, the actuator movements are enlarged by the 50- $\mu$ m micro-lenses, fabricated in our clean room. The free-space beam is then received by a TIA-APD array with an aperture on top of a rotation stage (PR01/M), therefore capable of controlling the angle of incidence of the incoming beam.

The lens radius was selected to optimize two key objectives: maintaining the desired beam divergence angle at  $2^\circ$ , and maximizing the scan angles close to the desired  $60^\circ$  FoV. In initial tests and simulations, the 50- $\mu$ m lenses demonstrated their adequacy in size. This size prevented the optical beam from reaching the lens edge, where significant beam distortions occur. Additionally, the lenses had a short focal length of 111  $\mu$ m, resulting in substantial beam movement magnification.

The signal is then sent to the Anritsu Error Detector (MP1764A) for counting bit error rate (BER) values. Signal-to-noise ratio (SNR) is measured by an Agilent Oscilloscope (MSO6104A). The steering angle is determined using a high-quality near-infrared (NIR) camera to measure a target positioned 40 cm away from the lens.

## Results and Discussions

Initially, we determined the maximum range of steering for the given setup, 0 to 20V for the horizontal movement. The actuator was set to the middle point and aligned with the centre of the camera. Subsequently, the voltage was varied from 0 to 20V and back to evaluate the movement linearity and the actuator hysteresis, which is the difference in the actuator position during the forward and return movement.

Figure 3 demonstrates a linear angle increase of the actuator from  $-13.7^\circ$  to  $+14.2^\circ$ , giving a total FoV of  $27.9^\circ$  on the horizontal X movement. However, the actuator shows hysteresis, of  $3.2^\circ$ , when its forward movement is compared to its return movement.

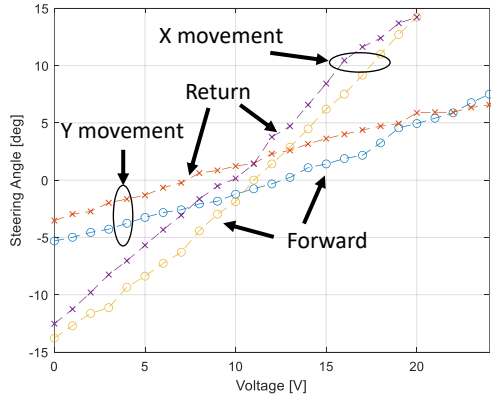


**Fig. 3:** Horizontal X and vertical Y movement of the actuators. Hysteresis can be observed in the actuator forward and return movement.

Similar hysteresis of  $2.7^\circ$ , can also be observed for the vertical Y movement, see also Fig. 3. In this case, the voltage sweep was increased to 24V max. For the Y movement, a linear but slow angle increase can be seen from  $-5.3^\circ$  to  $+7.5^\circ$ , giving a FoV of  $12.8^\circ$ . This slow increase is attributed to the fact that the vertical actuator holds the additional weight of the horizontal actuator, at the same time having less flexibility because of the fixtures.

For measuring the speed of the proposed concept, a camera with a frame rate of 26 frame per second was used. The speed was calculated by first setting the voltage to zero, starting the camera recording, subsequently setting the voltage to the maximum, and finally analysing the resulting frames. The vertical speed was measured at  $219^\circ/\text{s}$  or equivalent to  $1.22\pi$  rad/s and the horizontal speed  $649^\circ$  or  $3.61\pi$  rad/s.

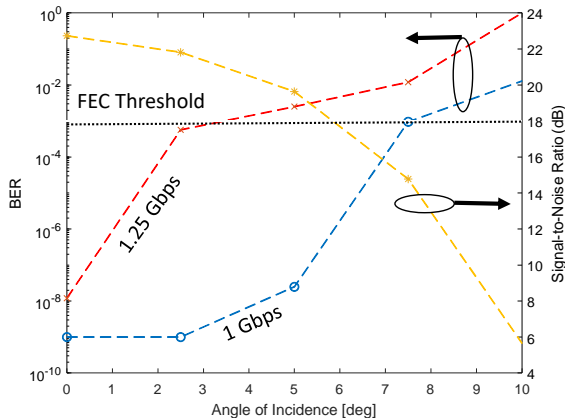


**Fig. 4:** BER and SNR performance versus steering angles of the piezoelectric beam steerer.

The BER and SNR performance were measured with the 750-MHz bandwidth receiver (Rx) on a swivel base. After each point, the base was turned  $2.5^\circ$ , allowing the evaluation of the signal deterioration in relation to the beam entry angle. We tested the data rates of 1 Gbps OOK and 1.25 Gbps OOK with the constant launching power with PRBS-9. The scanning range of the

beam steerer is set to  $0$  to  $10^\circ$  to be in line with the FoV of the OWC Rx. The measured BER and SNR values are depicted in Fig. 4. BER values of 1.25 Gbps decrease sharply when compared to those of 1 Gbps due to the narrow bandwidth of OWC Rx. Regarding the scanning angle, one can observe that the scanning performance is largely limited by the FoV of the Rx, and not by the beam steerer. This can be seen by the fact that the SNR values significantly decrease when approaching the  $10^\circ$  incident angle of the Rx, which is the maximum FoV of the employed Rx. Pre-FEC error-rates of  $10^{-3}$  can be reached until  $7-8^\circ$  incident angle to Rx. Therefore, we can conclude that the beam property of the proposed MEMs cantilever beam steerer works very well for relatively wide transmission angles, at least exceeding the  $20^\circ$  full FoV. However, more investigation will be done to design a lens magnifier for an optimum scan angle of  $60^\circ$  FoV.

## Conclusions

This work proposes the use of MEMs cantilevers equipped with micro-lenses and piezoelectric actuators to steer optical beams fast towards the position of indoor (mobile) wireless users. This concept is attractive due to the low loss, compact size, and relatively ease to be implemented.

The lens-assisted beam-steering, using a pair of piezoelectric actuators, demonstrated continuous steering with a  $27.9^\circ$  FoV in the horizontal plane, and a  $12.8^\circ$  in the vertical plane. The asymmetry is attributed to added weight and fixtures from the horizontal actuator. Both, horizontal and vertical, planes have a fast-steering capability of  $3.61\pi$  and  $1.22\pi$  radians per second, respectively. Although showing the actuator's hysteresis, the transmission angle is a linear function of the applied voltage on the actuators.

BER values for various transmission angles can be made error-free at small penalties w.r.t the cell center. An automatic control system should be developed for user movement tracking at walking speeds and evaluation in a realistic indoor communication testbed is required to demonstrate its beam pointing capability.

## Acknowledgments

The authors thank Simone Cardarelli from MicroAlign for the piezoelectric actuators.

This work is supported by the Netherlands Organization for Scientific Research (NWO) under the grant number 12128 Optical Wireless Superhighways: Free Photons.

## References

- [1] "Chapter II Frequencies" in Radio Regulations - Articles - Edition of 2020 Geneva, Switzerland: ITU, 2022, Ch. 2, pp 39-198
- [2] T. Koonen, "Indoor Optical Wireless Systems: Technology, Trends, and Applications," *J. Light.*

- Technol.*, vol. 36, no. 8, pp. 1459–1467, Apr. 2018, doi: [10.1109/JLT.2017.2787614](https://doi.org/10.1109/JLT.2017.2787614).
- [3] M. Z. Chowdhury, Md. T. Hossan, A. Islam, and Y. M. Jang, "A Comparative Survey of Optical Wireless Technologies: Architectures and Applications," *IEEE Access*, vol. 6, pp. 9819–9840, 2018, doi: [10.1109/ACCESS.2018.2792419](https://doi.org/10.1109/ACCESS.2018.2792419).
- [4] "Laser safety," *Wikipedia*. May. 01, 2023. [Online]. Available: [https://en.wikipedia.org/w/index.php?title=Laser\\_safety&oldid=1103030189](https://en.wikipedia.org/w/index.php?title=Laser_safety&oldid=1103030189)
- [5] C. Hoy, J. Stockley, J. Shane, K. Kluttz, D. McKnight, and S. Serati, "Non-Mechanical Beam Steering with Polarization Gratings: A Review," *Crystals*, vol. 11, no. 4, p. 361, Mar. 2021, doi: [10.3390/cryst11040361](https://doi.org/10.3390/cryst11040361).
- [6] T. Koonen, J. Oh, K. Mekonnen, Z. Cao, and E. Tangdiongga, "Ultra-High Capacity Indoor Optical Wireless Communication Using 2D-Steered Pencil Beams," *J. Light. Technol.*, vol. 34, no. 20, pp. 4802–4809, Oct. 2016, doi: [10.1109/JLT.2016.2574855](https://doi.org/10.1109/JLT.2016.2574855).
- [7] S. Cardarelli, N. Calabretta, R. Stabile, K. Williams, X. Luo, and J. Mink, "Wide-Range 2D InP Chip-to-Fiber Alignment Through Bimorph Piezoelectric Actuators," in *2018 IEEE 68th Electronic Components and Technology Conference (ECTC)*, San Diego, CA, USA: IEEE, May 2018, pp. 1124–1129. doi: [10.1109/ECTC.2018.00172](https://doi.org/10.1109/ECTC.2018.00172).
- [8] S. Chang, X. Guo, and X. Ni, "Optical Metasurfaces: Progress and Applications," *Annu. Rev. Mater. Res.*, vol. 48, no. 1, pp. 279–302, Jul. 2018, doi: [10.1146/annurev-matsci-070616-124220](https://doi.org/10.1146/annurev-matsci-070616-124220).
- [9] R. Fatemi, A. Khachaturian, and A. Hajimiri, "A Nonuniform Sparse 2-D Large-FOV Optical Phased Array With a Low-Power PWM Drive," *IEEE J. Solid-State Circuits*, vol. 54, no. 5, pp. 1200–1215, May 2019, doi: [10.1109/JSSC.2019.2896767](https://doi.org/10.1109/JSSC.2019.2896767).
- [10] M. J. Escuti and W. M. Jones, "A polarization-independent liquid crystal spatial light modulator," presented at the SPIE Optics + Photonics, I.-C. Khoo, Ed., San Diego, California, USA, Aug. 2006, p. 63320M. doi: [10.1117/12.681213](https://doi.org/10.1117/12.681213).
- [11] J. M. Pavia, M. Wolf, and E. Charbon, "Measurement and modeling of microlenses fabricated on single-photon avalanche diode arrays for fill factor recovery," *Opt. Express*, vol. 22, no. 4, p. 4202, Feb. 2014, doi: [10.1364/OE.22.004202](https://doi.org/10.1364/OE.22.004202).